# The Role of Integrated Modeling in the Design and Verification of the James Webb Space Telescope

Gary E. Mosier[a], Joseph M. Howard[a], John D. Johnston[a], Keith A. Parrish[a], T. Tupper Hyde[a], Mark A. McGinnis[b], Marcel Bluth[b], Kevin Kim[b], and Kong Q. Ha[c]
[a]NASA Goddard Space Flight Center, Greenbelt, MD
[b]Swales Aerospace, Beltsville, MD
[c]Jackson and Tull, Chartered Engineering, 7375 Executive Place, Seabrook MD

## ABSTRACT

The James Web Space Telescope (JWST) is a large, infrared-optimized space telescope scheduled for launch in 2011. System-level verification of critical optical performance requirements will rely on integrated modeling to a considerable degree. In turn, requirements for accuracy of the models are significant. The size of the lightweight observatory structure, coupled with the need to test at cryogenic temperatures, effectively precludes validation of the models and verification of optical performance with a single test in 1-g. Rather, a complex series of steps are planned by which the components of the end-to-end models are validated at various levels of subassembly, and the ultimate verification of optical performance is by analysis using the assembled models. This paper describes the critical optical performance requirements driving the integrated modeling activity, shows how the error budget is used to allocate and track contributions to total performance, and presents examples of integrated modeling methods and results that support the preliminary observatory design. Finally, the concepts for model validation and the role of integrated modeling in the ultimate verification of observatory are described.

Keywords: JWST, optics, integrated modeling, image quality, telescope, verification, validation

## 1. INTRODUCTION

The JWST is a large, near- and mid-infrared optimized space telescope under development by a team consisting of NASA, a prime contractor team led by Northrop Grumman Space Technology (NGST), the European Space Agency (ESA), and the Canadian Space Agency (CSA). Development of the JWST is led by the JWST project at NASA Goddard Space Flight Center (GSFC). JWST will have an 18-segment, 6.5-meter primary mirror and will reside in an L2 Lissajous orbit. The observatory, Fig. 1, is composed of three main elements: an Optical Telescope Element (OTE), an Integrated Science Instrument Module (ISIM), and a spacecraft consisting of the spacecraft bus and sunshield. The OTE consists of the hexagonal primary mirror segment assemblies (PMSAs), a secondary mirror support structure (SMSS), an aft optics assembly (AOS), and a backplane structure that supports the preceding subsystems. The ISIM consists of three science instruments – Near-infrared camera (NIRCAM), Near-infrared multi-object spectrograph (NIRSPEC), Mid-infrared camera (MIRI) – and a fine guidance sensor (FGS), all of which are mounted to a common ISIM bench structure that is, in turn, kinematically mounted to the OTE backplane. The spacecraft provides pointing and housekeeping functions for the observatory, while the deployable sunshield provides passive radiative cooling and stray light control for the telescope and science instruments.

The passive thermal control system, featuring the multi-layer sunshield plus large radiators on the ISIM enclosure, cools the OTE and ISIM to approximately 40K, with the detectors cooled further to 8K by a dewar. Fine pointing performance at HST-like levels (7 mas) is achieved through the use of the FGS and a two-axis fine steering mirror (FSM) plus a two-stage passive vibration isolation design to mitigate reaction wheel disturbances. Diffraction-limited performance of the observatory is achieved and maintained via periodic active control of the telescope. The active control uses NIRCAM images to sense the wavefront errors, followed by commands to the PMSA actuators. There are seven actuators per segment: six in a hexapod configuration for rigid body positioning, and a seventh actuator for radius of curvature correction. In between corrections, performance relies on passive structural stability, along with the fine pointing and vibration isolation systems.

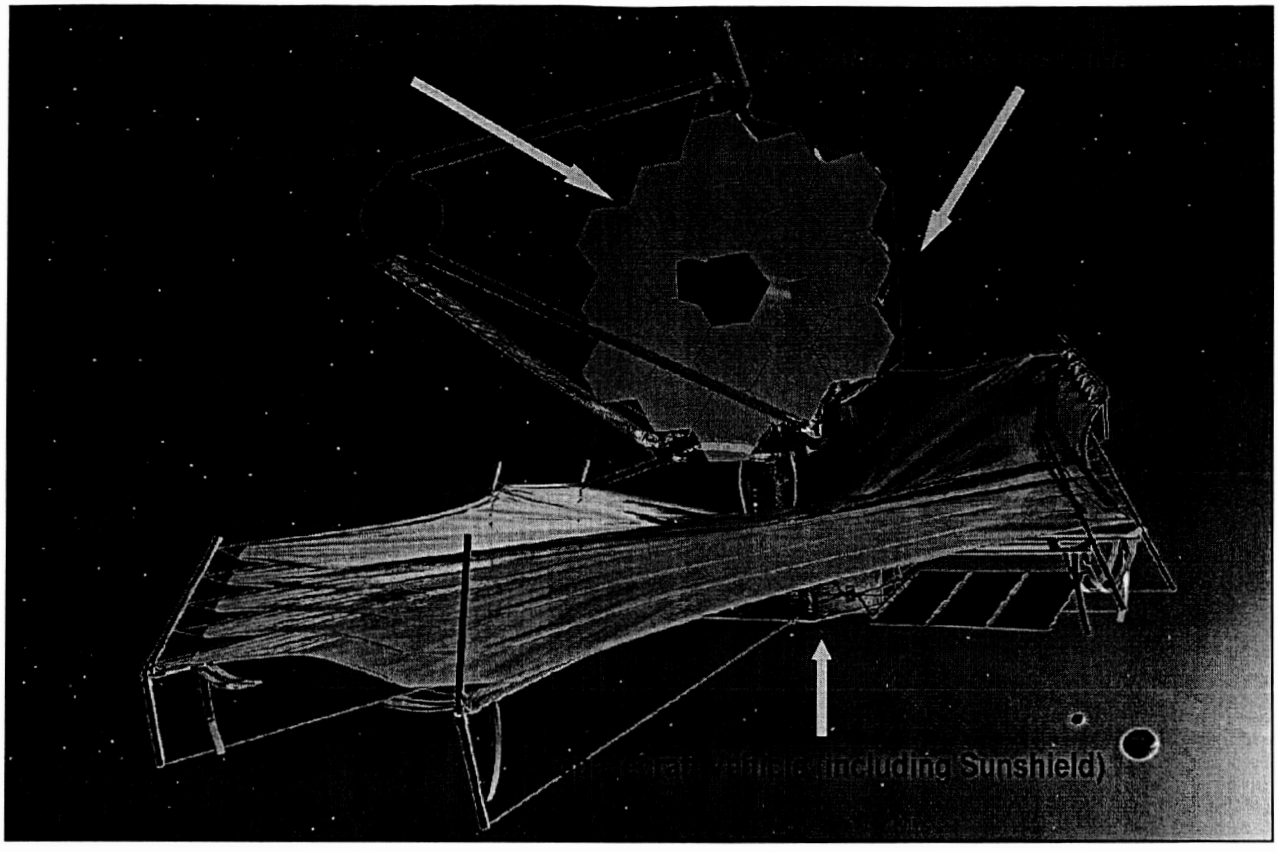


Figure 1: JWST Observatory Architecture

## 2. OPTICAL REQUIREMENTS, ERROR BUDGETS, AND INTEGRATED MODELING

Multi-disciplinary engineering analysis, or integrated modeling, will play a critical role in the development and verification of this observatory. Integrated modeling primarily supports observatory system-level design factors that relate to high-level optical requirements for image quality and sensitivity (signal-to-noise ratio for faint objects). This paper deals with some of the aspects of integrated modeling related to the following image quality requirements:

- Strehl Ratio: $\geq 0.8$, $\lambda = 2$ μm (caps total wavefront error at 150 nm root-mean-squared (rms))
- Encircled Energy (EE): 74% at R = 150 mas, $\lambda = 1$ μm (constrains mid-spatial frequency wavefront errors)
- PSF Anisotropy: $\leq 5\%$ variation in orthogonal axes (constrains asymmetric wavefront errors)
- EE must be stable over short (24 hours) and long (~30 days) periods

The requirements given govern the performance of the OTE combined with the Near-infrared instruments. Similar requirements exist at longer wavelengths for the combination of OTE plus Mid-infrared instrument.

Performance (error) budgets are maintained to control allocations to the various subsystems that comprise the JWST observatory. These budgets are traceable to the high level optical requirements. The image quality requirements are recast as requirements on wavefront error. These allocations may be roughly classified as belonging either to manufacturing and assembly of the optics, initial alignment of the optics following launch including the periodic recalibrations, or opto-mechanical stability between recalibrations. The opto-mechanical stability allocations may be further sub-classified as "drift" (long-term variations between individual exposures) or "vibration" (fast dynamics and image motion that smear individual exposures).

For each entry in the budget, individual wavefront error allocations are made to low-, mid-, and high frequency (spatial, i.e. cycles/aperture) bands in order to simultaneously meet the multiple constraints given above. For instance, wavefront errors in any band affect Strehl ratio, but only errors in the mid- and high frequency bands affect Encircled Energy.

One could view the primary integrated modeling activities falling out of the image quality requirements as consisting of three distinct multi-disciplinary analysis efforts: (1) thermal distortion, or STOP (Structural-Thermal-Optical), analysis to estimate alignment and figure drift due to observatory re-pointing, (2) image motion/jitter analysis, to estimate the blurring and distortion due to uncompensated pointing and vibration, and (3) wavefront sensing and control, to estimate the post-calibration alignment and figure errors. This paper will concern itself only with the first of these.

The applications of integrated modeling will change over the program life cycle. In the formulation and requirements definition phase, a strawman design was developed to address the high-level mission requirements, goals, and constraints. The role of integrated modeling was to validate this design concept by showing that the conceptual design met the requirements with margin, subject to reasonable assumptions, and that initial sub-allocations to observatory elements and sub-systems were also reasonable. Following a series of requirements reviews at the various program levels (mission, observatory, telescope, instruments), the modeling activity has aligned with the architecture/design activity in a series of cycles, each of 6-9 month duration. There will be multiple design cycles between major program review milestones. At the beginning of each cycle, a baseline design (or several as long as significant design trades are active) will be "frozen", and the set of multi-disciplinary analyses will be executed to verify that the baseline design(s) for that cycle meet the optical system requirements, with margin. The analysis will not only produce predictions of nominal design performance, but will also address uncertainties in performance due to variability in design parameters, material properties, and the environment. Finally, integrated modeling will be the basis for the ultimate optical performance verification of the as-built observatory, as no end-to-end test of the entire observatory under flight-like conditions is feasible. Verification of the image quality requirements will be "by analysis" rather than "by test".

## 3. STRUCTURAL-THERMAL-OPTICAL (STOP) ANALYSIS

### 3.1. STOP Analysis Process

The performance budget dictates that the opto-mechanical stability of the JWST observatory be maintained within specification between recalibrations. The current performance budget allocates 25 nmrms WFE for alignment drift and 32 nmrms for figure drift. This leads to a RSS total allocation of 41 nmrms for drift stability. One of the uses of STOP analysis on the JWST project is to estimate alignment figure drift due to thermal distortions resulting from re-pointing (slewing) of the observatory. The multi-disciplinary STOP analysis process described here links thermal, structural, and optical models in a "bucket-brigade" fashion to predict the response of the system to a slew maneuver about the pitch axis. The process is outlined schematically in Figure 2. The process begins with a thermal analysis to determine steady-state temperature distributions for a range of observatory orientations. The orientations corresponding to hot and cold cases are identified, and temperature results are "mapped" from the thermal to the structural model. The structural model is then used to predict distortions resulting from thermal loading, and displacements of optically important surfaces are "mapped" to the optical model. Finally, perturbations from the structural analysis results are introduced to the optical model and the optical performance of the system is predicted. The focus of current analyses is to predict the change in optical performance due to a "worst-case" slew between the hot and cold observatory orientations. This slew case results in the maximum thermal distortion and hence bounds the expected performance range. Further details regarding the discipline models and analyses are provided in the following sections. The models and corresponding results described here were developed by the prime contractor team and delivered to the government team at the time of the observatory system requirements review (SRR).

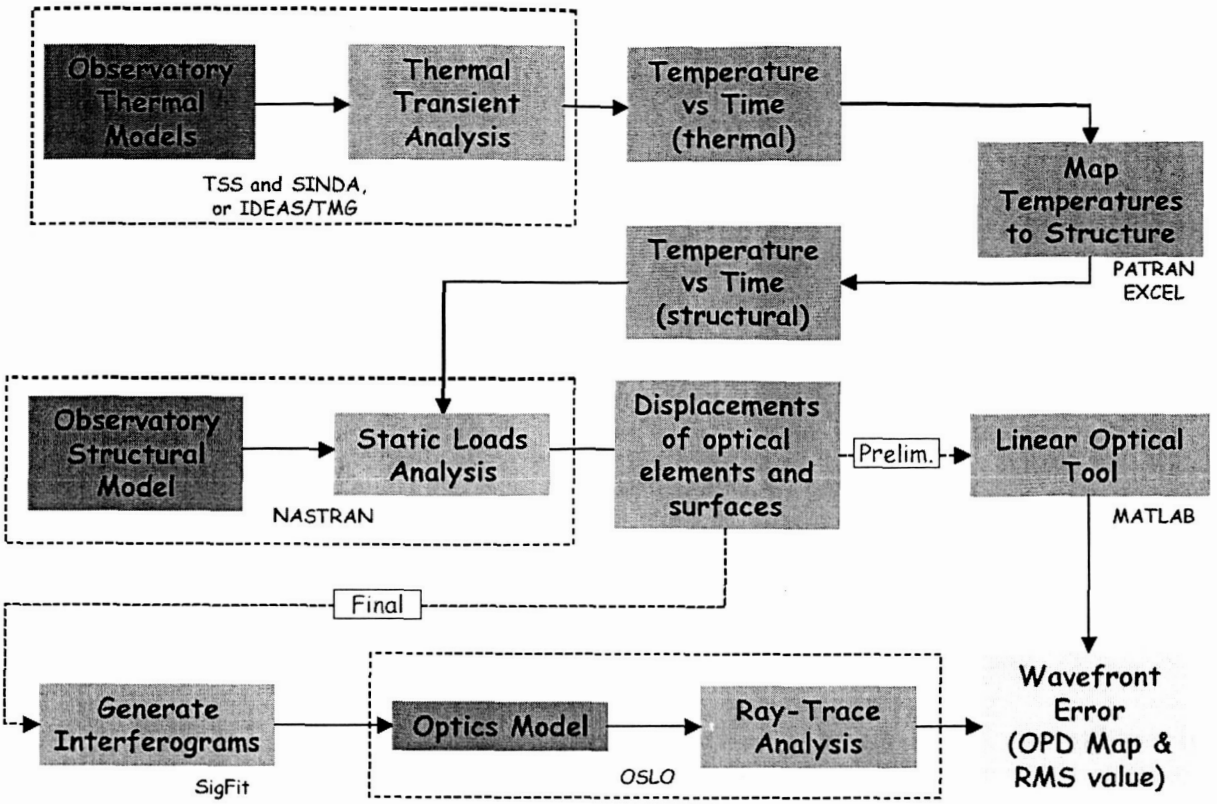


Figure 2: STOP analysis process map

### 3.2. Description of Current Models

The JWST observatory thermal model consists of a TSS radiation model and a SINDA/G thermal network math model. The TSS model consists of 3 major parts: the geometry file that defines shape/size/location/surface properties, the "radk" file consisting of radiative conductors calculated and generated using the geometry file and ray tracing methods, and the heat rate run that calculates and generates heat rates related to solar and infrared energy. SINDA/G is used to predict the temperature of the system using the data set from the TSS runs, user generated linear conductive coupling, and necessary heater/power dissipations. Note that only the steady state response is considered here, and optical properties used in all thermal models are end of life (EOL) properties. Based on temperatures obtained from the thermal math model and the model topology contained in the geometric thermal model, a table of coordinates and corresponding temperatures is obtained for hand-off to the structures discipline, a process referred to as temperature mapping. The process used to map temperatures for the results presented in the following section involves fitting a function to the thermal results, then mapping this function to the structural model mesh.

The NASTRAN structural model of the deployed observatory is shown in Figure 3(a). The model contains sufficient detail in the optical support structure areas to represent important thermo-structural effects without undue detail that would slow trade studies. Temperature-dependent values for the coefficient of thermal expansion are included in the model. NASTRAN requires that the tabulated values are "secant" CTE values. Two successive linear static analysis runs, both from the reference temperature state, are required to perform the on-orbit stability analysis. The applied temperature loads are the initial and final on-orbit temperature states, and the difference between these two states represents the effect of the slew. Structural deformations are input as perturbations to the optical model to assess optical performance. Mappings were required between the structural model and two different optical models (see discussion in the following section): an optical ray trace model and a linear optical model. An interferogram file is used as the interface between the NASTRAN structural model and the OSLO optical ray trace model for mapping primary mirror

deformations. The interface between the structural model and the linear optical model is a matrix of six degree of freedom motions, three translations and three rotations, for 22 optics (18 primary mirror segments, secondary mirror, tertiary mirror, fine steering mirror, and image surface).

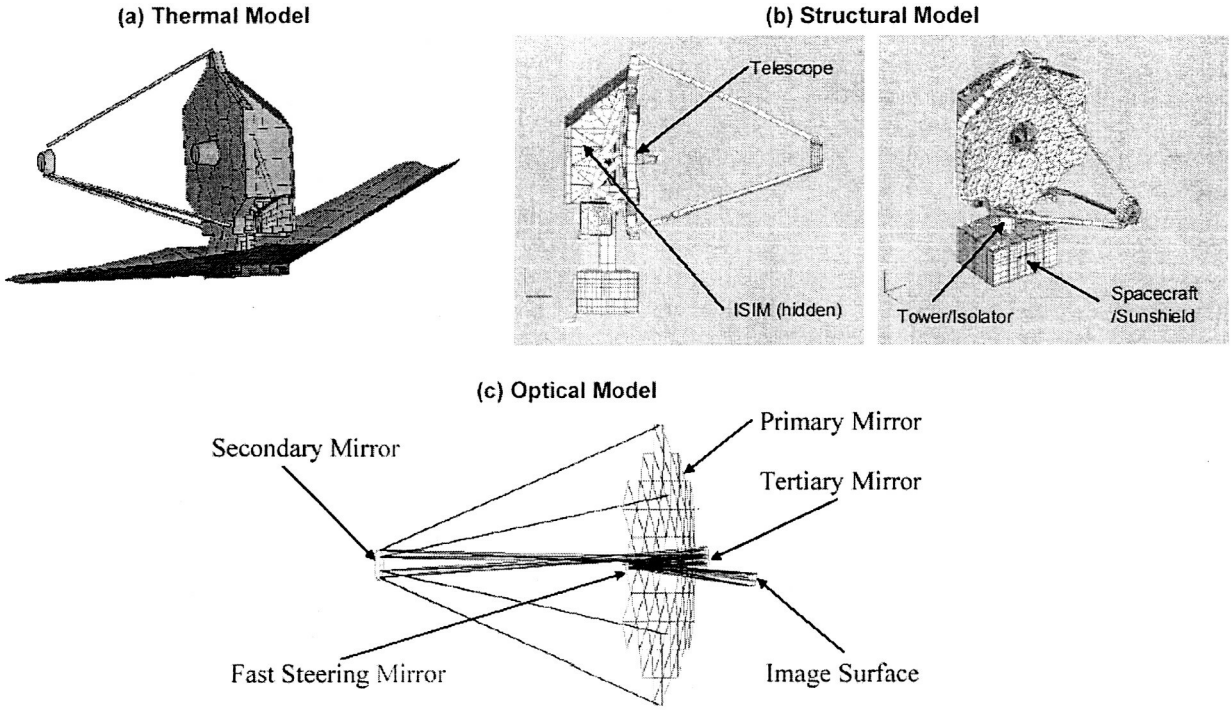


Figure 3: Discipline models for STOP analysis: (a) thermal geometric model, (b) structural finite element model, and (c) optical ray trace model.

The JWST government analysis team uses two different models to assess optical performance. The first is an optical ray trace model, and the second is a linear optical model that is used primarily for first-order perturbation studies. Ray tracing for this analysis is performed using either of two optical prescriptions delivered from the prime contractor: one having a monolithic primary mirror surface, and the other having a segmented primary (non-sequential surface). The former is generally used for analyses that assume the primary mirror is aligned perfectly, while the latter is used to more accurately model alignment procedures and other more detailed analyses. Both models are delivered in OSLO optical design software lens format. Rigid body perturbations due to thermal (or other) loads are applied to either optical model by changing the coordinates defining the location of each optic, while deformations to the optical surfaces are applied to each surface using an interferogram file. The approach taken for the linear optical model involves performing all ray tracing in advance through the system with a single known rigid body perturbation applied to each surface and each degree of freedom. This generates linear sensitivities, which are used as transfer matrices converting rigid body motions of optical components to absolute image motion at the detector and wave front error induced due to the misaligned components. The linear optical model can be briefly described as a first-order Taylor expansion of the optical path lengths of a grid of rays traced through the system, uniformly spaced at the entrance pupil. The variables expanded upon are the rigid body degrees of freedom (DOF) for each optical component in the system. The primary figure of merit for the optical analysis is root-mean-square wave-front error (RMS WFE), evaluated at the exit pupil of the system for the central field point. This is also referred to as a map of optical path differences, or "OPD map". If the rate of change of the perturbation is much slower than the exposure time or the ability for the fine guidance system to track the image, as it will be for typical thermal influences, then the RMS WFE is evaluated with the best-fit plane removed.

### 3.3. Current STOP Analysis Results

Figure 4(a) presents the steady-state temperature profile for the hot case (-15° pitch angle) illustrating primary mirror (PM) and backplane (BP) structure temperatures. The hot case is defined by the hottest average PM temperature among the cases studied. The plot indicates that for the hot case the maximum PM temperature is 58.3 K and the minimum temperature is 35.2 K. Note that the PM temperature gradient is primarily in the V3 direction with the hot side nearest the sunshield. Also note that the backplane structure has a temperature gradient that is similar albeit at a slightly higher temperature than the PM. Of interest in assessing the operational WFE stability of the telescope is the worst case temperature change as the observatory slews about the pitch axis. Figure 4(b) presents a plot of the worst case delta temperature profile (hot case – cold case), where the cold case is for a -45° pitch angle. The average change in temperature between states is approximately 0.3 K. The maximum change in temperature between states is less than 0.5 K over the entire PM and BP with the peak change occurring nearest the sunshield.

Figure 4(c) presents results from the structural model illustrating the deformations resulting from a change in temperature corresponding to the worst-case slew defined by the thermal analysis. Peak total displacements are on the order of 200 nm and occur in the secondary mirror support structure. The magnitude of the total displacements exhibited by the primary mirror (primary mirror segments plus backplane support structure) is on the order of 50 nm. Of interest in assessing wavefront error are the primary mirror surface normal displacements. NASTRAN results were post-processed using the Sigfit software package to obtain surface normal displacements with rigid body motions removed. The RMS value of the surface normal displacements is 8 nm and the peak-to-valley value is 42 nm. The structural model predicts that while the backplane support structure is the main contributor to primary mirror deformations, the PMSA's also make a significant contribution. Note that since the change in primary mirror temperature between states is greater near the sunshield, the PMSA's on that side of the primary mirror undergo larger motions than the PMSA's opposite the sunshield.

Results from the optical models with perturbations based on structural deformations resulting from the worst-case slew case are presented in this section. Optical performance predictions for RMS WFE are broken down into three spatial frequency bands: low (< 5 cycles per aperture), mid (>5 and <35 five cycles per aperture), and high (>35 cycles per aperture). These contributions are calculated in such a way that when RSS'ed they equal the total WFE. Optical results below are presented as total RMS WFE followed by the frequency decompositions. Figure 4(d) presents a map of the optical path difference evaluated at the exit pupil of the system for the central field point from the ray trace model. The RMS WFE is 18.2 nm (Low=17.8 nm, Mid=6 nm, High=2 nm) and a peak-to-valley WFE is 89 nm. The linear optical model shows good agreement with the ray trace model. Qualitatively the OPD maps are very similar, and the RMS WFE predicted by the linear optical model is within 20% of that predicted by the ray trace. The analytical results from the ray trace and linear optical models show that the observatory currently meets an RSS total allocation of 41 nm,rms for drift stability with ample margin. Future studies, outlined in the following section, will explore the sensitivity of these nominal results.

## 4. MODEL VALIDATION PLANS

### 4.1. Thermal Model Validation

Ideally, the JWST observatory thermal model would be validated by a system level thermal balance test of the flight observatory in its fully deployed operational configuration. However, this is not realizable when considering JWST's unprecedented scale and cryogenic operating temperatures. Even if such a test could be performed, it would only serve to determine the thermal performance of the observatory and would occur too late to validate models that are currently being used as input to the optical stability analysis. These unique circumstances and the reliance on thermal modeling necessitate a unique and thorough approach to thermal model validation and quality control. There are two key elements to JWST thermal model validation. The first element involves independent thermal modeling utilizing different personnel and analysis tools. In lieu of test data, two separate independent models are currently used to predict thermal performance. While not a substitute for actual tests, this independent modeling effort serves to build confidence in model predictions and uncovers modeling oversights and numerical errors related to specific modeling tools and

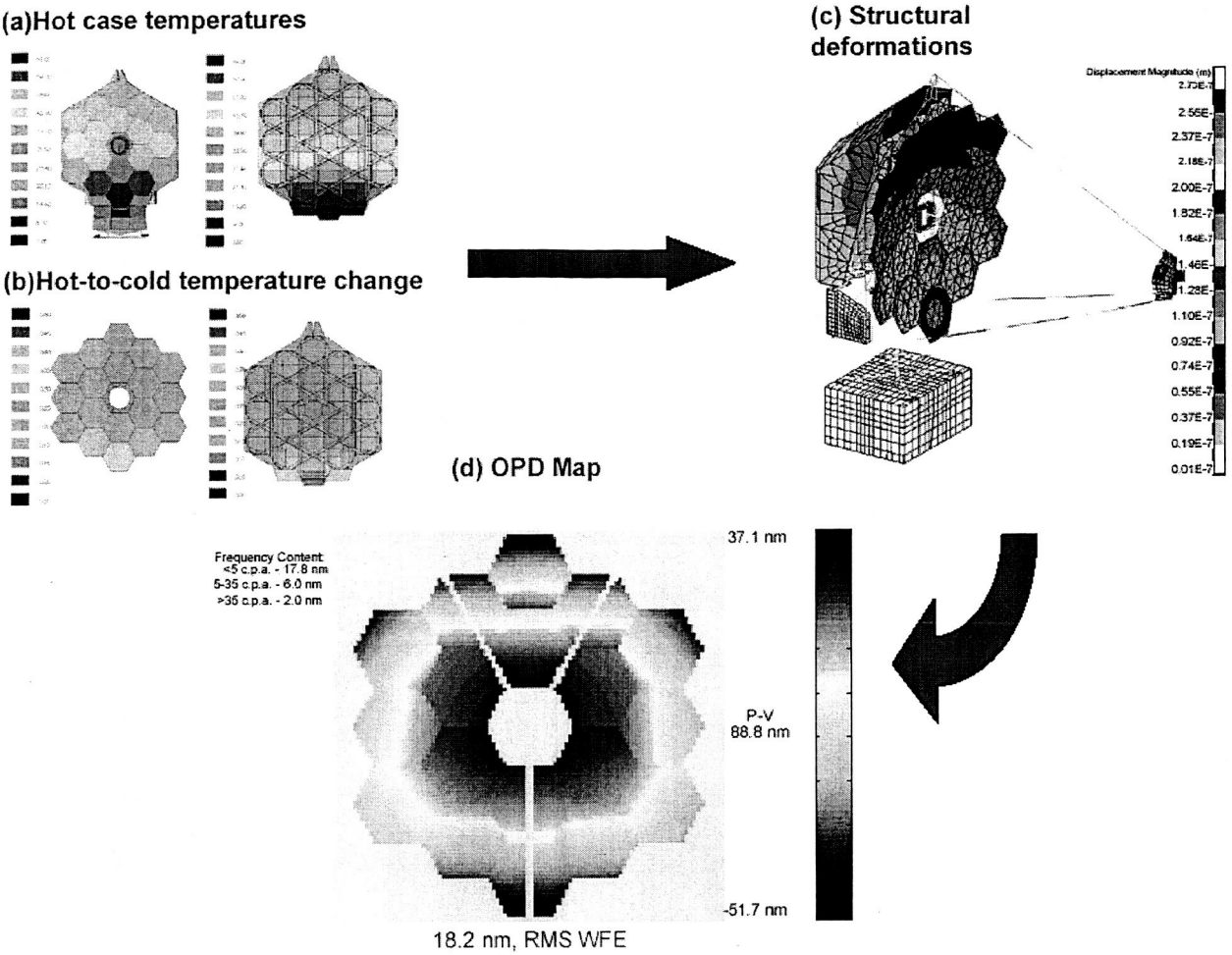


Figure 4: Representative Results from SRR STOP Analysis: (a) Delta temperature profile ('Hot-Cold' case), (b) Structural deformations, and (c) OPD map from ray trace.

methodologies. Complimentary to the independent modeling effort is a comprehensive set of thermal tests at various levels of JWST assembly. These tests are performed over a period of several years with each test providing portions of the information needed to validate the full-up observatory thermal model.

Figure 5 illustrates the various thermal tests that will serve to validate the overall observatory thermal model. Dates are not shown but preliminary developmental tests are occurring now. High level system tests occur much later in the 2009-2010 time frame. Thermal model validation is broken down into the verification of the thermal models of the individual observatory elements. Each observatory element's model validation is further broken down. The OTE and ISIM have the most extensive and numerous amount of thermal testing. For the ISIM, developmental tests of materials and key thermal control components are performed first. On a parallel path instrument level tests are performed to validate the instrument thermal models. Similarly for the OTE, material characterization and composite backplane thermal testing is performed first. The other key element in the observatory cryogenic thermal control system is the large deployed sunshield. Since the flight sunshield is too large to be deployed and thermal vacuum tested, a smaller scale high-fidelity thermal test model of the sunshield is constructed and tested in parallel with the ISIM and OTE developmental and instrument level tests. The thermal model of the spacecraft bus, which houses the star trackers that must be maintained in tight alignment with the cryogenic side fine guidance sensor, is validated via a more typical thermal balance test of the flight article.

In addition to these tests that serve to validate element level thermal models, there are currently three identified system level tests that will validate and measure the subtle but critical thermal interactions between the elements. The IEC, which houses room temperature electronics in close proximity to the cryogenic telescope and instruments, will radiate large amounts of heat on the cryogenic side of the observatory. In addition, the warm spacecraft bus and sunshield core will also radiate significant and detrimental heat to the cryogenic side. In order to better validate the models' prediction of these key radiative interfaces, two tests, an IEC specific and bus core thermal test are envisioned. The full-up flight test of the OTE and ISIM, in the Plumbrook thermal chamber at NASA's Glenn Research Center, is also viewed as a system test due to the critical thermal interaction of various elements that are tested there. It should also be mentioned that for the OTE and ISIM, flight unit testing is always preceded by thermal tests on engineering test units.

Throughout this long thermal test program, thermal model inputs are continually updated based on test results. The goal is to continually increase model confidence and verify thermal requirements serially as the observatory is constructed over the next several years. Although some tests are only currently conceptualized, the goal is to perform key tests early in the program such that any necessary design changes can be implemented in a meaningful time frame so as not to delay launch. It should be noted that although there are extensive and numerous tests, the cumulative and simultaneous thermal interaction of all of the elements is never verified. The risk of this 'piecemeal' verification approach is currently being quantified. One mitigation approach currently being studied is a thermal balance test of a smaller scale thermal model of the entire deployed observatory. If found to be viable, the sub-scale sunshield test would be enhanced to include high-fidelity thermal simulators of the other observatory elements.

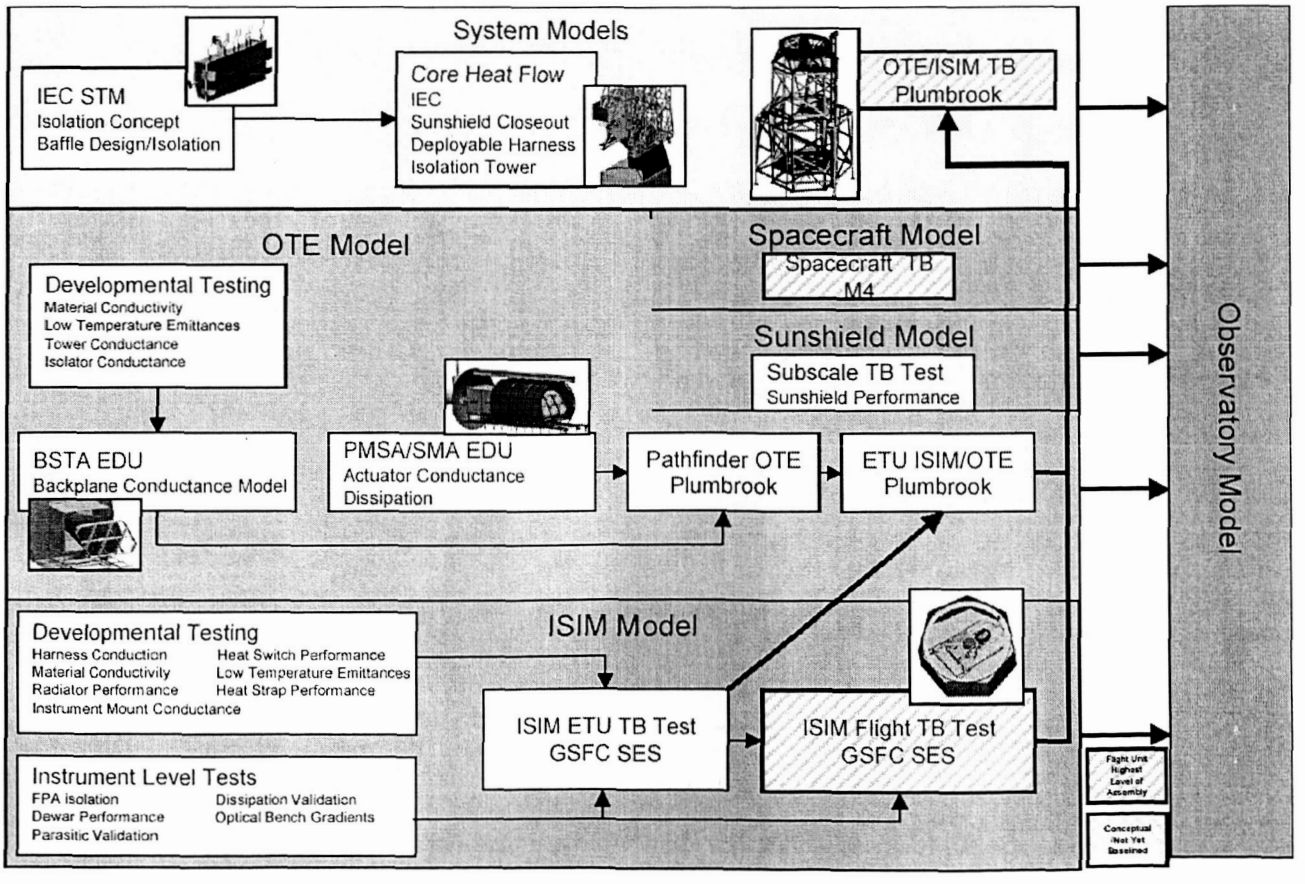


Figure 5: Thermal Model Validation for On-Orbit Thermal Stability

### 4.2. Structural Model Validation

A process will be established for structural models used to predict on-orbit thermal stability in which the models are progressively validated through correlation with tests, beginning with basic material characterization tests and followed by tests at successively higher orders of assembly. The first step involves basic material characterization tests to establish values for the elastic properties and thermal expansion coefficients over the operating temperature range. At the next level assembly, composite tubes and joint assemblies will be subjected to stiffness and thermal distortion tests to verify structural building block models. At the next level of assembly, structural sub-elements will be subject to thermal distortion and opto-mechanical testing at operating temperature. Thermal distortion tests are planned at this level to validate high-fidelity models for the ISIM and OTE composite structures. Test articles will consist of 2-D and 3-D frames structures representative of sections from the primary mirror backplane and ISIM bench structures. The backplane stability test article (BSTA) test is one of the key thermal stability risk reduction activities currently being pursued by the project. Note that this is currently foreseen as the critical level of assembly for validating the composite structures models, since tests at higher levels of assembly will be primarily focused on optical performance. Additionally, opto-mechanical tests will be performed on the PMSA's, SMSS, AOS, and Science Instrument (SI) subsystems. The next level of assembly involves testing that will validate built-up models of OTE and ISIM observatory elements. At this level of assembly, cryogenic optical performance tests will be completed on both ETU/Pathfinder and Flight structures. Finally, cryogenic optical performance tests will be completed at the system level on a combined OTE/ISIM structure.

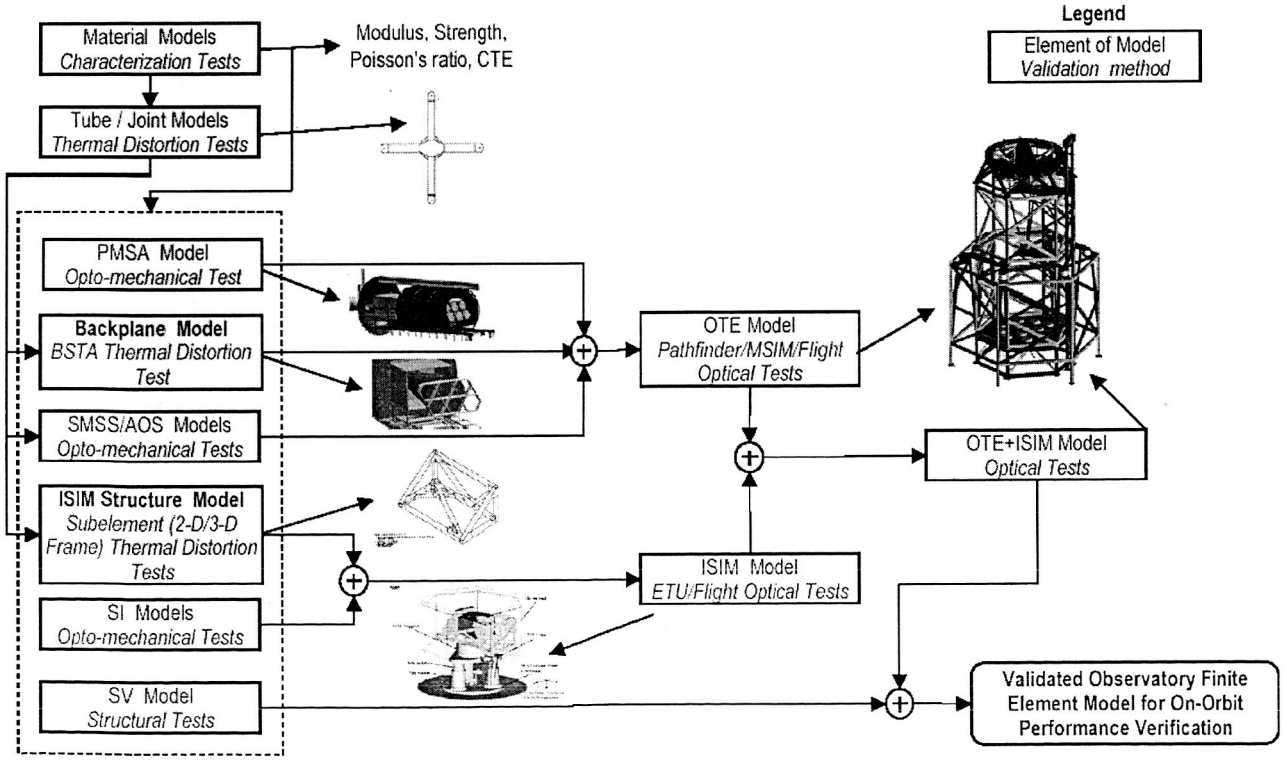


Figure 6: Structural Model Validation for On-Orbit Thermal Distortion

### 4.3. System Model Validation

A similar multi-stage process is envisioned to verify the integrated dynamics and controls models. Structural testing in the form of a modal survey will occur at various levels of subassembly. There will be no modal test of the entire observatory in the deployed configuration due to the sheer size and need to provide an overwhelming amount of supporting structure for gravity offload. Additional tests will occur in cryogenic facilities in order to verify the damping of the structures, as a follow on to cryogenic damping tests of materials. Component/Subsystem tests of the reaction wheels, reaction wheel isolators, OTE tower isolator, attitude control sensors, FGS and FSM will anchor the models of the primary pointing and vibration disturbances as well as their compensation/attenuation.

The final step in the validation of the integrated STOP model, and in the verification of system-level optical performance, involves optical testing that takes place at multiple levels. All optical components, and major sub-assemblies such as instruments, will undergo testing to characterize the as-built prescriptions. This testing provides the optical model with the information to characterize artifacts of the manufacturing and polishing stages, artifacts that produce residual errors in the mid- and high spatial frequency bands that, in turn, degrade encircled energy. An example would be the testing of the primary mirror segments as depicted in Figure 7.

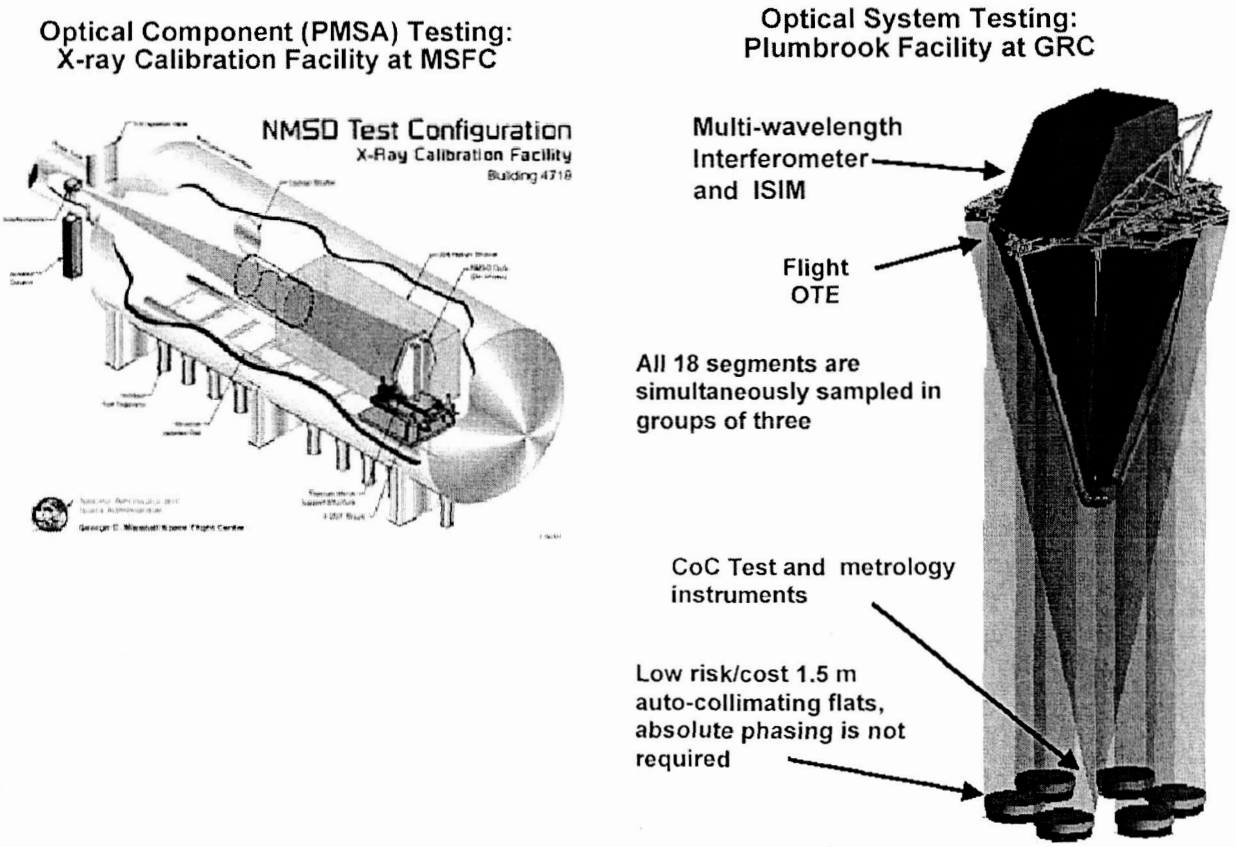


Figure 7: Optical Testing and Model Validation at the Component and System Levels

Figure 7 also depicts the system-level optical tests at the Plumbrook facility. This cryogenic test integrates the component-level optical measurements with several additional measurements. As shown, this is an end-to-end test that includes the flight OTE and ISIM. The entire wavefront sensing and control process will be verified, and the image-based wavefront sensor provides one measurement of the phase errors. Other measurements include a center-of-curvature test in which a source located in the center of the auto-collimating flats illuminates the entire primary mirror, and a multi-wavelength double pass interferometer (DPI) test that provides additional phase error information. The

sampled aperture phase map from the wavefront sensor is combined with the information obtained in the other tests, correlated with the component-level tests performed prior to Plumbrook, and then the effects of the Plumbook metrology (e.g. the auto-collimating flats) and test-procedures (e.g. to account for double-pass effects) are subtracted. The result, as depicted in Figure 8, is a reconstruction of the full aperture phase map. These data verify the performance of the static (manufacturing, alignment, figure) terms in the optical performance budget. It is up to the validated integrated model to provide the verification of the remaining (drift, vibration, image motion) terms in the budget, and here the tests at Plumbrook provide an additional anchor to the integrated model.

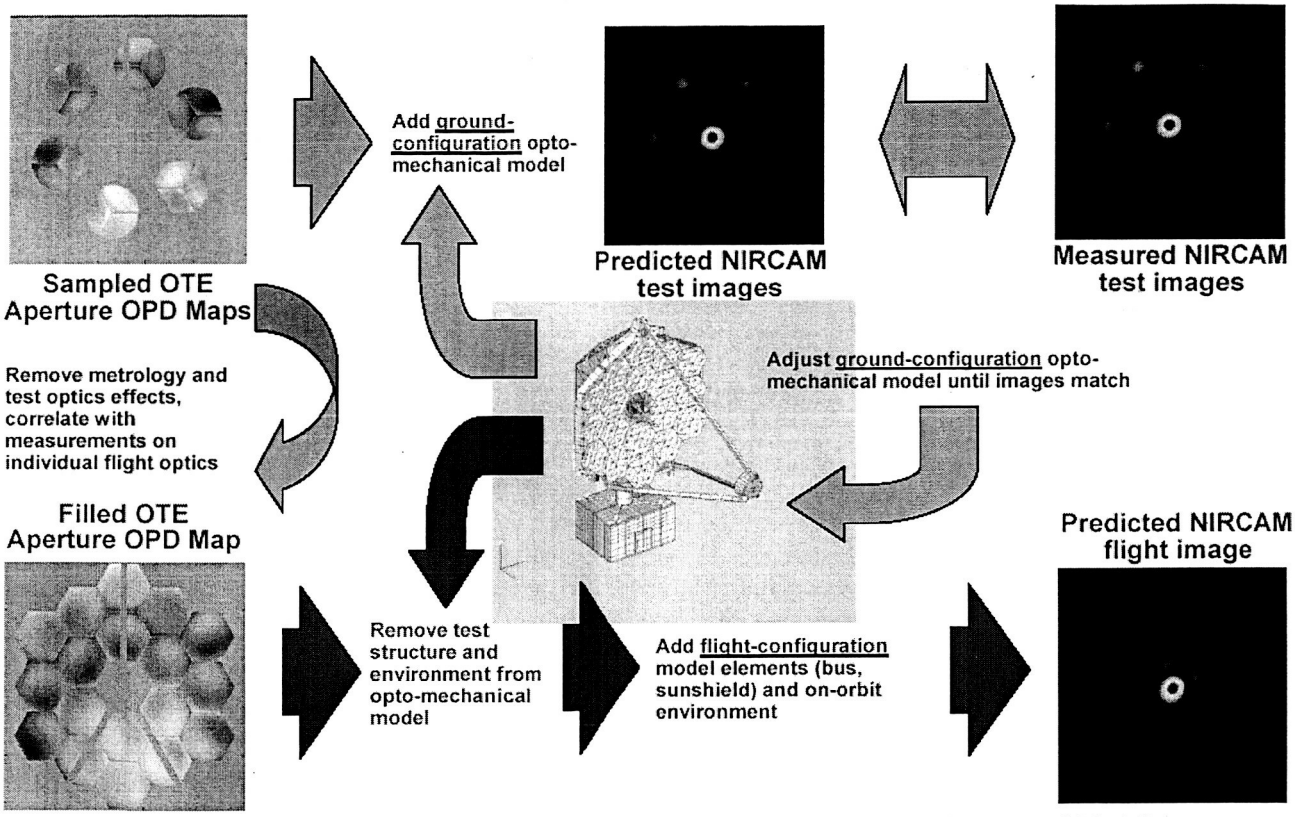


Figure 8: Performance Verification Combining Sampled Aperture Testing and Integrated Modeling

The optical measurements will occur over periods of hours and days, during which time the temperature of the observatory will be monitored with the flight thermocouples. Additional metrology in the test tower and cryogenic chamber will provide information on the seismic inputs and the thermal boundary conditions. Combined with the optical measurements, a series of predicted sampled aperture images can be correlated with actual images obtained with the NIRCAM. This correlation allows for a final correction of the OTE/ISIM jitter and STOP models. Following this step, the validated OTE/ISIM model is extracted from the system model of the Plumbrook configuration, and the missing elements of the flight configuration (spacecraft, sunshield) and flight environment are added. The integrated STOP and jitter models are then used to verify that the observatory meets the performance allocations for drift, vibration, and image motion.

## 5. SUMMARY

System-level verification of optical performance requirements for JWST will rely on integrated modeling to a considerable degree. In fact, the ultimate verification is by analysis, not by test, as it is not feasible to test the observatory as a whole under anything resembling flight-like conditions. These conditions must be recreated via validated, high fidelity models. And as it is not feasible to verify the observatory by test, it is not feasible to validate the

models using a single test. A complex series of tests are planned by which the components of the integrated models are validated at various levels of subassembly. These component models are then assembled for the final verification by analysis. Here, JWST is merely a harbinger of what is to come. Observatories of similar and even larger size are in the planning stages or even under development, and verification-by-analysis will be the only reasonable option. In order to mitigate the risks associated with this approach, the systems engineering philosophy must call for robust, correctable-in-situ designs. Advanced analysis techniques to efficiently and accurately predict parametric sensitivity and uncertainty in performance need to be developed. And model accuracy, and the process to verify it, must be established during system-level requirements development and allocation.

## 6. REFERENCES


1. Nella, J., "James Webb Space Telescope (JWST) observatory architecture and performance," SPIE Astronomical Telescopes and Instrumentation Conference, June 2004, SPIE 5487-23.
2. Joseph M. Howard, "Optical modeling activities for the James Webb Space Telescope (JWST) project: I. The linear optical model," Proc. SPIE Int. Soc. Opt. Eng. 5178, 82 (2004).
3. Howard, J.M., et al, "Optical Modeling Activities for the James Webb Space Telescope (JWST): 2. Determining Image Motion and Wavefront Error Sensitivities for a Segmented Optical System Over An Extended Field," SPIE Astronomical Telescopes and Instrumentation Conference, June 2004, SPIE 5487-142.
4. Hyde, T.H., et al, "Integrated Modeling Activities for the James Webb Space Telescope (JWST): Optical Jitter Dynamics Analysis," SPIE Astronomical Telescopes and Instrumentation Conference, June 2004, SPIE 5487-122.
5. Johnston, J., et al, "Integrated modeling activities for the James Webb Space Telescope: Structural-Thermal-Optical Analysis," SPIE-5487-123.
6. Mosier, G., Parrish, K., Femiano, M., Redding, D., Kissil, A., Papalexandris, M., Craig, L., Page, T., and Shunk, R., "Performance Analysis Using Integrated Modeling", NGST Monograph No. 6, August 2000.
7. Mosier, G., Femiano, M., Ha, K., Bely, P., Burg, R., Redding, D., Kissil, A., Rakoczy, J. and Craig, L., "An Integrated Modeling Environment for Systems-level Performance Analysis of the Next Generation Space Telescope," SPIE Vol. 3356, Space Telescopes and Instruments V, 1998.
8. Mosier, G., Femiano, M., Ha, K., Bely, P., Burg, R., Redding, D., Kissil, A., Rakoczy, J. and Craig, L., "Fine Pointing Control for a Next Generation Space Telescope," SPIE Vol. 3356, Space Telescopes and Instruments V, 1998